T-spline Parameterization of 2D Geometries Based on the Meccano Method with a New T-mesh Optimization Algorithm

J.I. López[1], M. Brovka[1], J.M. Escobar[1], J.M. Cascón[2], and R. Montenegro[1]

[1] University Institute for Intelligent Systems and Numerical Applications in Engineering, SIANI, University of Las Palmas de Gran Canaria, Spain
{jilopez,mbrovka,jmescobar,rmontenegro}@siani.es
http://www.dca.iusiani.ulpgc.es/proyecto2012-2014

[2] Department of Economics and History of Economics, Faculty of Economics and Management, University of Salamanca, Spain
casbar@usal.es

Summary. We present a new method, based on the idea of the meccano method and a novel T-mesh optimization procedure, to construct a T-spline parameterization of 2D geometries for the application of isogeometric analysis. The proposed method only demands a boundary representation of the geometry as input data. The algorithm obtains, as a result, high quality parametric transformation between 2D objects and the parametric domain, the unit square. First, we define a parametric mapping between the input boundary of the object and the boundary of the parametric domain. Then, we build a T-mesh adapted to the geometric singularities of the domain in order to preserve the features of the object boundary with a desired tolerance. The key of the method lies in defining an isomorphic transformation between the parametric and physical T-mesh finding the optimal position of the interior nodes by applying a new T-mesh untangling and smoothing procedure. Bivariate T-spline representation is calculated by imposing the interpolation conditions on points sited both on the interior and on the boundary of the geometry. The efficacy of the proposed technique is shown in several examples.

Keywords: T-spline parameterization, simultaneous mesh untangling and smoothing, meccano method, isogeometric analysis, quadtree.

1 Introduction

An open problem in the context of isogeometric analysis [1, 2, 7] is how to obtain a spline parameterization of a complex computational domain from the CAD description of its boundary.

J. Sarrate & M. Staten (eds.), *Proceedings of the 22nd International Meshing Roundtable*,
DOI: 10.1007/978-3-319-02335-9_4, © Springer International Publishing Switzerland 2013

Parameterization is suitable for analysis if it does not have self-intersection, i.e., the Jacobian is strictly positive at any point of the computational domain. Moreover, in order to expect a high accuracy in numerical results it is necessary to obtain a good quality parameterization. Orthogonality and uniformity of isoparametric curves are desirable for the tensor-product structured parameterization. This task is not trivial and can be very time-consuming. For application of IGA it is essential to have an efficient method to construct T-spline parameterization. In the present work we investigate this problem for planar geometries.

There are only a few works addressing this problem. In [24], the parameterization is found by solving a constraint optimization problem for the control points of a planar B-spline surface. Constraints are defined by imposing injectivity sufficient conditions in terms of control points, and the optimization consists in the minimization of some energy functions in order to reach a good orthogonality and uniformity of the parametric mapping. Another similar technique was proposed by these authors in [25]. They use a harmonic mapping obtained by solving an optimization problem for the control points. Additional term is added to the objective function in order to improve the quality where needed. The use of harmonic mapping is a common characteristic of several works dealing with 2D and 3D parameterization methods [18, 19, 20].

In this paper, we propose a different approach where the parameterization is accomplished by transforming isomorphically a T-mesh from the parametric domain to the physical one. The construction of this transformation is mainly based on a simultaneous T-mesh untangling and smoothing procedure.

As far as we know, the only case of performing mesh untangling and smoothing procedure for a T-mesh, in order to construct T-spline representation of 3D domains, was described in [23, 26]. They remove tangled elements by maximizing the worst Jacobian. Smoothing is performed by moving each node towards the mass center of its neighboring elements. Another strategy for optimizing a grid with hanging nodes was described in [3]. Mesh optimization is carried out via a global grid smoothing functional based on shape quality and size control metrics for the elements of the mesh. Some constraints are imposed on the position of hanging nodes in order to place them in the middle point of their edge.

In our previous works [11, 12] we constructed the physical T-mesh of the solid using a volumetric parameterization obtained by deforming a tetrahedral mesh of the solid. In general, this approach does not provide an optimal T-mesh quality in the sense of its uniformity and orthogonality. Now, we propose a different approach where the optimization is applied directly to the T-mesh.

Our technique is simple and easy to implement. Satisfactory results are obtained with low computational effort for a variety of complex geometries.

This paper is organized as follows. In next section we describe the main steps of the proposed algorithm. In section 3 we explain the process of boundary parameterization and the construction of T-mesh adapted to the singularities of the object boundary. Section 4 describes the simultaneous T-mesh untangling and smoothing

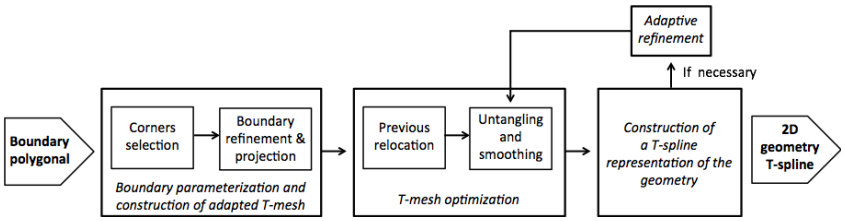

Fig. 1 General scheme of the T-spline parameterization method

procedure that leads to the construction of a high quality T-mesh of the object. The modeling of the geometry by means of bivariate T-splines is developed in section 5. A quality improvement strategy, based on adaptive refinement, is described in the section 6. In section 7 we illustrate the results of the application of the algorithm to some 2D domains. Finally, in section 8 we present the conclusions and set out some challenges.

2 General Scheme of the Method

In this section we summarize the proposed method in order to facilitate its understanding. Some ideas of the method are taken from our previous works on mesh untangling and smoothing and the meccano method [4, 5, 8, 10, 21, 22], but they have been adapted to the requirements of the present work.

The algorithm includes the following stages:

1. *Boundary parameterization and construction of an adapted T-mesh:* A bijective correspondence between the input boundary of the object and the boundary of the parametric domain is defined. Then, an adapted T-mesh is generated by refining the initial mesh in order to approximate the geometry with a prescribed tolerance. During this process, the boundary nodes of the parametric domain are mapped to the boundary of the object.
2. *T-Mesh optimization:* We relocate the inner nodes of the T-mesh by applying a simultaneous mesh untangling and smoothing procedure. A previous relocation of the inner nodes is accomplished in order to facilitate this task.
3. *Construction of a T-spline representation of the geometry:* The T-spline parameterization is obtained by imposing interpolation conditions. As interpolation points, we take the vertices of the physical T-mesh obtained after the optimization process and other necessary additional points.
4. *Adaptive refinement to improve the mesh quality:* If the quality of the T-mesh is not satisfactory, we apply an adaptive refinement in order to increase the degree of freedom in the areas with high distortion. Then, we return to step 2 and repeat the process until reaching a good T-spline parameterization.

The T-mesh used in this work has a balanced quadtree structure: all refinements are performed by dividing a cell into 4 equal cells and a procedure of balancing

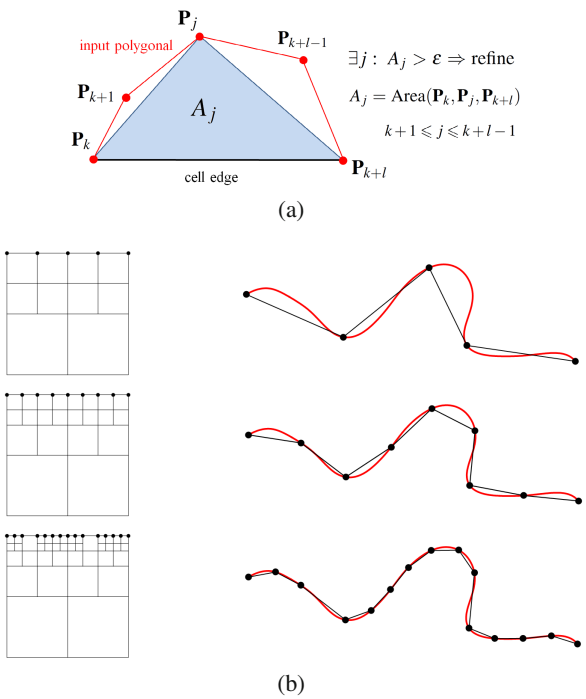

Fig. 2 (a) Illustaration of the refinement criterion used for the boundary approximation. (b) Construction of the adapted T-mesh in order to approximate the object boundary with a desired tolerance. Example of the boundary approximation corresponding to the upper edge of the unit square. Red line represents the input boundary.

is applied in order to allow just one hanging node per edge. The input boundary representation is given by a polygonal, however it could be given by B-spline curves.

A scheme of the algorithm is shown in Fig. 1.

3 Boundary Parameterization and Construction of an Adapted T-mesh

In order to define a parametric mapping between the input boundary polygonal of the object and the boundary of the parametric domain, the unit square, we have to select four points of the polygonal that will correspond to the four corners of the square. These points divide the input polygonal into four parts that are mapped via chord-length parameterization into its corresponding edge of the square. The selection of the corners must be appropriate. Namely, the corners should be situated in convex areas of the input boundary polygonal, where the inner angle formed by the polygonal in these points is less than 180°. Obviously, the optimal value of this angle is 90°. At present this selection is carried out by the user.

Next, we construct an adapted T-mesh that approximates the input boundary with a prescribed tolerance ε. To do that, an approximation error is calculated for each boundary cell and the cell is refined if this error is greater than ε. A cell refinement produces a new boundary point that is projected over the input boundary polygonal, obtaining a more accurate approximation of the geometry. As approximation error, we evaluate the area of the triangles formed by the cell edge in the physical space and each vertex of the input polygonal approximated by this edge. A cell is refined if there is at least one triangle whose area exceeds ε, see Fig. 2(a). The process of construction of an adapted T-mesh is illustrated in Fig. 2(b).

As result of this stage, the position of the boundary nodes in the physical domain are known and the position of the inner nodes will be defined by means of the T-mesh optimization procedure developed in next section. Fig. 3(a) shows an example of the adapted parametric T-mesh constructed in this stage and, Fig. 3(b), illustrates the resulting tangled T-mesh of the physical domain that will be optimized.

4 T-mesh Optimization

The key of the proposed method lies in the optimization procedure that allows to obtain a high quality physical T-mesh used to construct the T-spline representation of the object.

It is preferable to perform a previous relocation of the inner nodes in order to reduce the computational effort during the optimization process. In the present work, we have used for this purpose Coons patch [6, 13] to define a surface that interpolates given boundary curves. This previous relocation procedure facilitates the untangling process, but in general does not obtain a satisfactory mesh quality and can produce self-intersections, as shown in Fig. 3(c). Therefore, it is essential to apply an efficient optimization algorithm.

4.1 Objective Function

The mesh optimization process is carried out by iterative relocation of each inner node of the mesh in such a way that the new position of the node improves the quality of the local submesh corresponding to this node. A local submesh is the set of all the elements connected with the movable or *free node*. The local objective function for a free node is based on algebraic shape quality metrics proposed by Knupp in [16, 17] for triangular and quadrilateral elements. Shape quality metric for a given triangle is defined in terms of the Jacobian matrix of the affine mapping from ideal triangle to the given one. This shape quality metric represents the deviation of the physical triangle from the ideal one. It attains its maximum value, 1, if the triangle is similar to the ideal one, and it equals 0 if the triangle is degenerated. The distortion metric of an element is defined as the inverse of its quality metric. In order to asses the quality of the local submesh for a given free node of a T-mesh, we

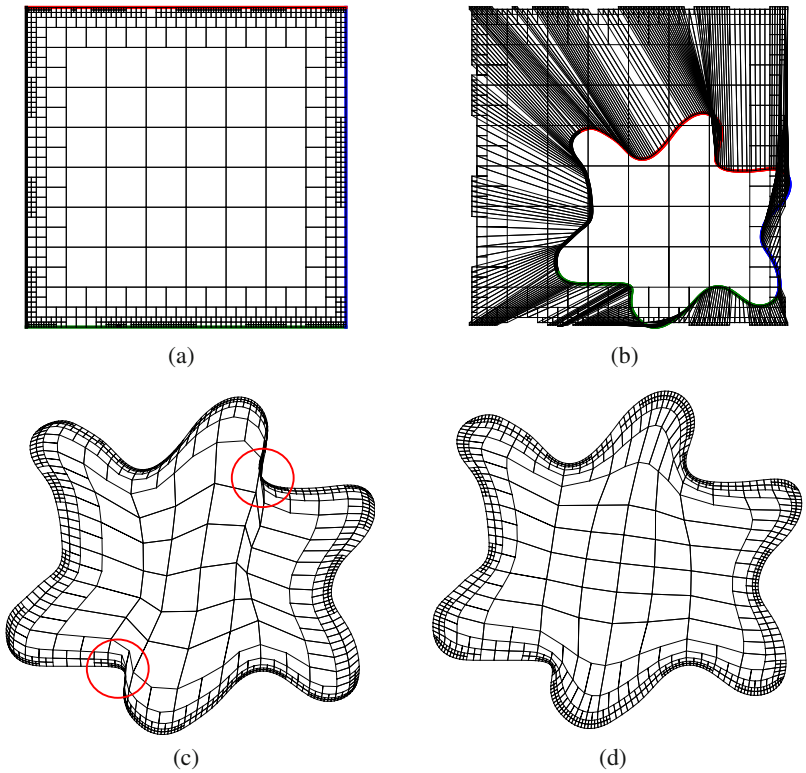

Fig. 3 Stages of the T-mesh construction for the Spot test model geometry. (a) Parametric T-mesh adapted to the boundary of the geometry; (b) tangled physical mesh after boundary mapping (the color bold lines represent the correspondence between parametric and physical boundaries); (c) previous relocation by using Coons patch, highlighting self-intersections; (d) optimized physical T-mesh.

have to decompose each neighboring cell into triangles and asses the quality of each triangle. For a T-mesh, this decomposition depends on the type of the free node. There are two types of free node: a regular node and a hanging node. The optimal position of each free node is determined by minimizing a local objective function. We define the objective function as a sum of shape distortion metrics of the triangles of the local submesh. For each triangle of the physical mesh, the corresponding triangle of the parametric mesh is used as its ideal element. Therefore, each cell of the physical mesh tends to have the same shape as its counterpart cell of the parametric mesh. Thus, repeating this procedure for all the inner nodes of the mesh, we achieve the physical mesh of the object is as similar to the parametric one as possible.

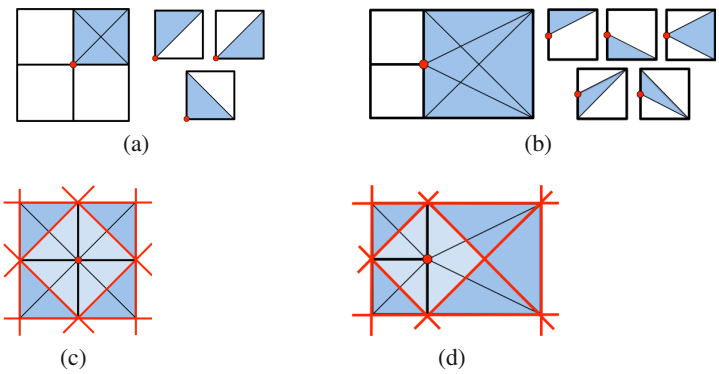

Fig. 4 Triangular decomposition of the free node local submesh, where the red point is the free node. (a) Regular node case, where each cell is decomposed in three triangles; (b) hanging node case, where five triangles are formed in the cell where the node generates a T-juntion; (c) barriers (red lines) and feasible region (light blue) induced by the 12 triangles in the objective function for a regular node; (d) barriers and feasible region induced by the 11 triangles in the objective function for a hanging node.

A regular node is surrounded by four cells with equal or different sizes. In order to perform the mesh improvement, the local submesh is decomposed in twelve triangles, three triangles per cell whose qualities depends on the position of the free node. Fig. 4(a) illustrates this decomposition and Fig. 4(c) shows the feasible region of the objective function.

In a hanging node case, the free node is surrounded by three cells and the local submesh is decomposed in eleven triangles. The cell in which the node forms a T-junction is decomposed in five triangles whose qualities depend on the position of the free node. Each one of the other two cells is decomposed in three triangles, as was described in the case of a regular node. Fig. 4(b) shows the decomposition of a local submesh for hanging node case and the feasible region of the objective function. Note that, for the ideal case shown in Fig. 4(d), the feasible region induced by these eleven triangles is the same as the one obtained after a refinement of the T-junction cell, see Fig. 4(c).

In order to define the objective function we introduce the following concepts.

Let T be a triangle whose vertices are given by $\mathbf{x}_k = (x_k, y_k)^T \in \mathbb{R}^2$, $k = 0,1,2$ and T_R be the reference triangle with vertices $\mathbf{u}_0 = (0,0)^T$, $\mathbf{u}_1 = (1,0)^T$ and $\mathbf{u}_2 = (0,1)^T$. If we choose $\mathbf{x}_0$ as the translation vector, the affine map that takes T_R to T is $\mathbf{x} = A\mathbf{u} + \mathbf{x}_0$, where A is the Jacobian matrix of the affine map referenced to node $\mathbf{x}_0$, and expressed as $A = (\mathbf{x}_1 - \mathbf{x}_0, \mathbf{x}_2 - \mathbf{x}_0)$.

Let consider that T_I is our ideal or target triangle whose vertices are $\mathbf{v}_0$, $\mathbf{v}_1$ and $\mathbf{v}_2$. If we take $\mathbf{v}_0 = (0,0)^T$, the linear map that takes T_R to T_I is $\mathbf{v} = W\mathbf{u}$, where $W = (\mathbf{v}_1, \mathbf{v}_2)$ is its Jacobian matrix. As the parametric and real meshes are topologically

identical, each triangle in the physical space has its counterpart in the parametric space.

Affine map that takes T_I to T is given by $\mathbf{x} = AW^{-1}\mathbf{v} + \mathbf{x}_0$, and its Jacobian matrix is $S = AW^{-1}$. Note that this weighted matrix S depends on the node chosen as reference, so this node must be the same for T and T_I. We can use matrix norms, determinant or trace of S to construct algebraic quality metrics of T. For example, the *mean ratio*, $q = \frac{2\sigma}{\|S\|^2}$, is an easily computable algebraic quality metric of T, where $\sigma = \det(S)$ and $\|S\|$ is the Frobenius norm of S. The maximum value of q is the unity, and it is reached when $A = \mu RW$, where μ is a scalar and R is a rotation matrix. In other words, q is maximum if and only if T and T_I are similar. Besides, any flat triangle has quality measure zero. We can derive an optimization function from this quality metric. Thus, let $\mathbf{x} = (x,y)^T$ be the position of the free node, and let S_m be the weighted Jacobian matrix of the m-th triangle connected to this free node. We define the objective function of $\mathbf{x}$, associated to an m-th triangle as

$$\eta_m = \frac{\|S_m\|^2}{2\sigma_m} \tag{1}$$

The local objective function used for mesh quality improvement is defined by means of the inverse of mean ratio quality metric of each triangle of the local submesh. The function to be minimized is given by

$$K(\mathbf{x}) = \sum_{m=1}^{M} \eta_m \tag{2}$$

where M is the number of triangles in the local submesh and S_m is the Jacobian matrix associated to the affine mapping from the *ideal* triangle to the physical one.

Objective function defined by Eq. (2) is appropriate to improve the quality of a valid mesh, but it does not work properly when there are inverted elements [14, 15]. In the previous work [8] we introduced a modified objective function K^*, where the untangling and smoothing are carried out in the same stage. This modified objective function K^* does not have singularities, it works as the original function K for the valid elements and tends to untangle the inverted and degenerated ones. This objective function is defined as

$$K^*(\mathbf{x}) = \sum_{m=1}^{M} \eta_m^* \tag{3}$$

being

$$\eta_m^* = \frac{\|S_m\|^2}{2h(\sigma_m)} \tag{4}$$

where $h(\sigma) = \frac{1}{2}(\sigma + \sqrt{\sigma^2 + 4\delta^2})$. Objective function K^* is smooth in $\mathbb{R}^2$, so the unconstrained optimization problem can be easily solved with any standard method.

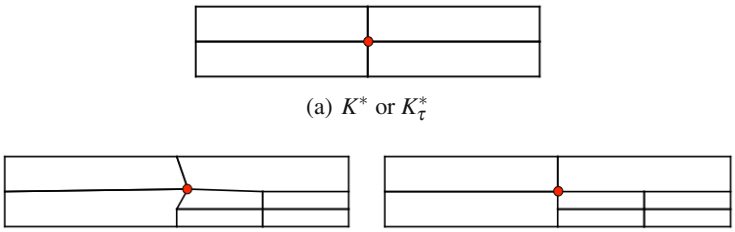

(a) K^* or K^*_τ

(b) K^* (c) K^*_τ

Fig. 5 Resulting meshes after optimization with different objective functions. (a) Orthogonal mesh using K^* or K^*_τ; (b) not satisfactory result for a non-conformal local submesh using K^*; (c) orthogonal mesh using weighted objective function K^*_τ.

In case of a conformal local submesh, the result obtained by minimizing the objective function K^* is, when possible, an orthogonal submesh, as shown in Fig. 5(a). However, not satisfactory result is obtained for a non-conformal submesh. In this case, two special situations can appear: a regular node surrounded by cells of different scales and a hanging node. In these situations, a variation in the position of the free node does not affect in the same way to the quality of the triangles of the local submesh. The objective function tends to form triangles as similar as possible to the reference ones, but the influence of the smaller cells are greater than the bigger ones. For example, in Fig. 5(b) it can be seen how the free node is moved toward the small cell and, therefore, the resulting mesh is not orthogonal.

This problem is solved by a modification of the objective function K^*, namely multiplying the terms of the objective function by appropriate weights.

4.2 Weighted Objective Function

The terms of the objective function K^* can be grouped according to the belonging to each cell of the local submesh. Each group is multiplied by an appropriated weight in order to avoid the mentioned problems in section 4.1.

For a regular node, the weighted objective function is

$$K^*_\tau(\mathbf{x}) = \tau_1 \sum_{m=1}^{3} \eta^*_m + \tau_2 \sum_{m=4}^{6} \eta^*_m + \tau_3 \sum_{m=7}^{9} \eta^*_m + \tau_4 \sum_{m=10}^{12} \eta^*_m \tag{5}$$

where each summation is the group associated to each cell and τ_i is the applied weight. We can prove that this weight is equal to the scale factor of the cell in the parametric space, but it has not been included due to space limitation of this paper. We assume that the smallest cells in the local submesh have scale factor $\tau = 1$ and the other cells can have scale factor $\tau = 2$ or $\tau = 4$, as illustrated in Fig. 6(a). Fig. 5(c) shows the resulting orthogonal mesh when these weights are applied.

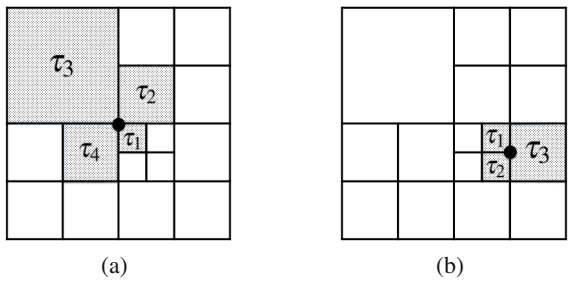

Fig. 6 Weights for the objective functions K_τ^*. (a) Regular node where $\tau_1 = 1$, $\tau_2 = \tau_4 = 2$ and $\tau_3 = 4$; (b) hanging node where $\tau_1 = \tau_2 = 1$ and $\tau_3 = \frac{8}{5}$.

A hanging node is surrounded by three cells as it was mentioned above. In this case, the weighted objective functions is

$$K_\tau^*(\mathbf{x}) = \tau_1 \sum_{m=1}^{3} \eta_m^* + \tau_2 \sum_{m=4}^{6} \eta_m^* + \tau_3 \sum_{m=7}^{11} \eta_m^* \tag{6}$$

Hanging node is a more particular case because its local submesh is decomposed in different types of triangles. To guarantee the orthogonality in the local submesh after optimization, we have determined that the weights are $\tau_3 = \frac{8}{5}$ for the cell where the node forms a T-junction and $\tau_1 = \tau_2 = 1$ for the other two cells, as shown in Fig. 6(b).

5 Construction of a T-spline Representation of the Geometry

In this section we describe the construction of T-spline representation for 2D geometries. We have to obtain a global one-to-one parametric transformation that maps the parametric domain into the physical domain $\mathbf{S} : \hat{\Omega} = [0,1]^2 \to \Omega$.

5.1 T-splines

In order to define T-spline basis functions of degree 3 over a given T-mesh in 2D, a local knot vector for both parametric directions should be assigned to each basis function R_α: $\Xi_\alpha = \left(\xi_{\alpha_1}, \xi_{\alpha_2}, \xi_{\alpha_3}, \xi_{\alpha_4}, \xi_{\alpha_5}\right)$, $H_\alpha = \left(\eta_{\alpha_1}, \eta_{\alpha_2}, \eta_{\alpha_3}, \eta_{\alpha_4}, \eta_{\alpha_5}\right)$. These knot vectors are inferred by traversing T-mesh edges. This basis function is associated to the central knot $(\xi_{\alpha_3}, \eta_{\alpha_3})$ that is called *anchor*. As we are using open knot vector structure, there are some blending functions that have the same anchor.

The T-spline blending functions that we use in this work are rational B-spline functions defined as

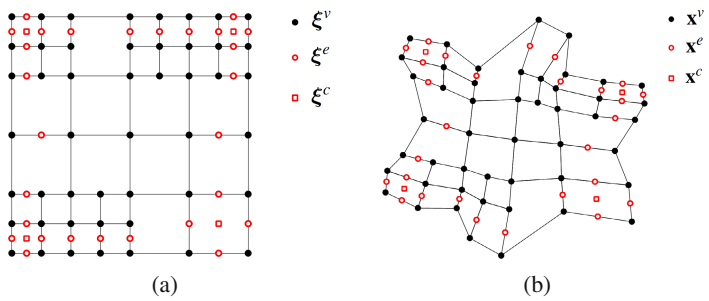

Fig. 7 Interpolation points in parametric and physical domains. (a) Parametric domain, $\boldsymbol{\xi}^v$ - vertices of the mesh, $\boldsymbol{\xi}^e$ - additional interpolation points situated on the edges of the mesh, $\boldsymbol{\xi}^c$ - additional points situated in the four corner cells; (b) interpolation points in physical domain.

$$R_\alpha(\boldsymbol{\xi}) = \frac{N_\alpha(\boldsymbol{\xi})}{\sum\limits_{\beta \in A} N_\beta(\boldsymbol{\xi})} \tag{7}$$

being $N_\alpha(\boldsymbol{\xi}) = N_\alpha^1(\xi) N_\alpha^2(\eta)$ the bivariate B-spline function defined over its local knot vectors $\boldsymbol{\Xi}_\alpha = \{\Xi_\alpha, H_\alpha\}$, and A is the index set of the basis spanned by T-mesh.

A detailed report about T-splines and their relationship with isogeometric analysis can be found in [2].

5.2 Interpolation

We build bivariate T-spline surface representation of our physical domain as lineal combination of T-spline blending functions

$$\mathbf{S}(\boldsymbol{\xi}) = \sum_{\alpha \in A} \mathbf{P}_\alpha R_\alpha(\boldsymbol{\xi}) \tag{8}$$

where $\mathbf{P}_\alpha \in \mathbb{R}^2$ is the control point corresponding to the α-th blending function.

Control points $\mathbf{P}_\alpha$ are found by imposing interpolation conditions. Assuming that the set of blending functions are linearly independent, we need as many interpolation points as blending functions.

As interpolation points, first of all, we use the *anchors* of the blending functions. Each *anchor* coincides with a T-mesh vertex, $\boldsymbol{\xi}_\alpha^v$, and its position in the physical space, $\mathbf{x}_\alpha^v$, was determined by the mesh optimization process.

According to the strategy adopted in the section 5.1, that leads to an open knot vector structure along the boundary of the mesh, the total number of blending functions is greater than the number of vertices of the T-mesh. Therefore, we have to take additional interpolation points. These additional points are associated to functions whose knot vectors Ξ_α or H_α contains exactly three repeated knots. We assign to each of these functions an interpolation point approximately sited where the function attains its maximum. The positions of these interpolation points in

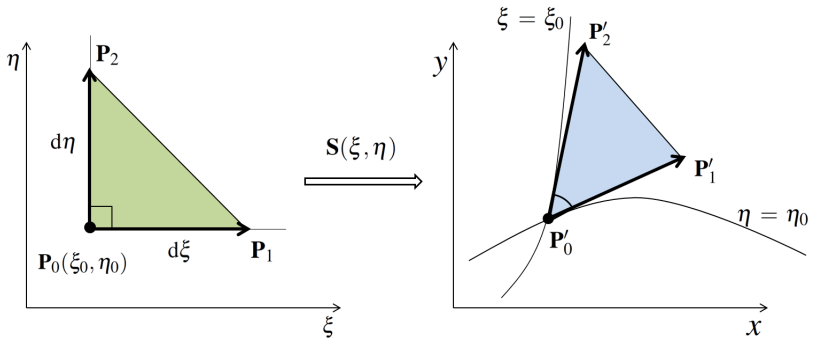

Fig. 8 Mean ratio Jacobian. A quality metric of the parametric mapping **S** at any point $\mathbf{P}_0$ in terms of the mean ratio of the triangle $\mathbf{P}'_0\mathbf{P}'_1\mathbf{P}'_2$.

parametric and physical spaces are shown in Fig. 7(a). For each additional interpolation point $\boldsymbol{\xi}_\alpha$, its position in the physical space, $\mathbf{x}_\alpha$, should be defined. The interpolation points $\boldsymbol{\xi}^e_\alpha$, situated at the mid point of an edge of the parametric mesh, are mapped to the mid point of the same edge of the physical T-mesh. The positions in the physical space of the four interpolation points $\boldsymbol{\xi}^c_\alpha$ situated in the center of the corner cells of the parametric mesh are determined by optimizing the local submesh formed after a fictitious quadtree partition of these cells.

Finally we solve the linear system of equations

$$\mathbf{x}_\beta = \mathbf{S}\left(\boldsymbol{\xi}_\beta\right) = \sum_{\alpha \in A} \mathbf{P}_\alpha R_\alpha\left(\boldsymbol{\xi}_\beta\right), \quad \forall \boldsymbol{\xi}_\beta,\ \beta \in A \tag{9}$$

where $\boldsymbol{\xi}_\beta$ are interpolation points in parametric space and $\mathbf{x}_\beta$ are their images in the physical space.

6 Adaptive Refinement to Improve the Mesh Quality

6.1 Mean Ratio Jacobian

Our objective is to get high-quality geometry parameterization suitable for isogeometric analysis. The parametric T-spline mapping of Eq. 8 is suitable for analysis if it has positive Jacobian in all the domain. High distortion of the geometry can produce a large variation of the Jacobian that can lead to a poor accuracy in the numerical results. Therefore, a good uniformity and orthogonality of the isoparametric curves are desired for the parametric mapping **S**.

A high quality of the optimized T-mesh is a necessary, but not sufficient, condition for a high quality of the T-spline mapping. It can happen that the Jacobian of the spline parameterization takes negative values even if all the cells of the T-mesh are valid. In order to assess the quality of the constructed parametric transformation we analyze the mean ratio Jacobian, given by

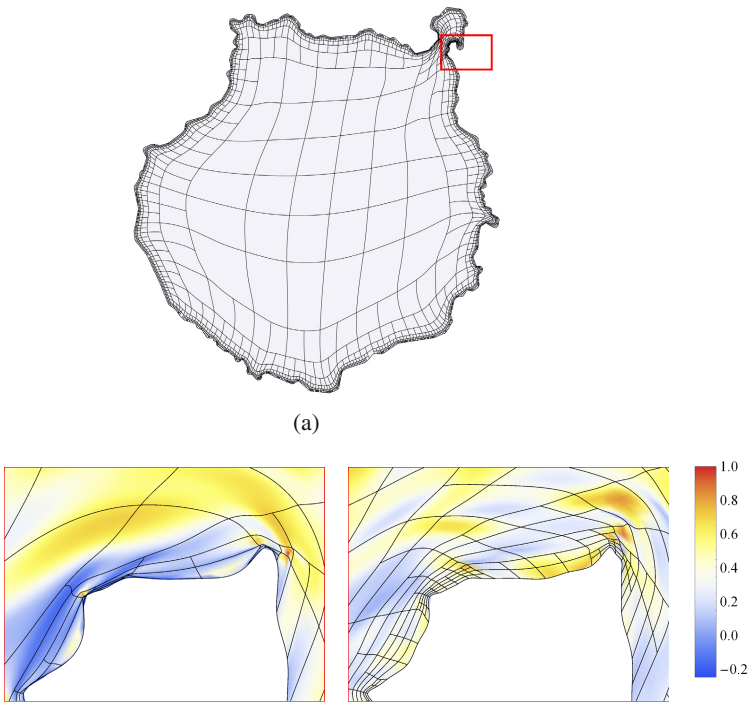

Fig. 9 Adaptive refinement strategy to improve the parametric transformation quality in Gran Canaria island domain. (a) T-spline representation of the domain; (b) initial T-spline parametrization and color map of its mean ratio Jacobian with negative values; (c) resulting T-spline parameterization after applying adaptive refinement and color map of its mean ratio Jacobian with no negative values.

$$J_r(\boldsymbol{\xi}) = \frac{2\det(J)}{\|J\|^2}, \tag{10}$$

where J is the Jacobian matrix of the mapping $\mathbf{S}$ at the point $\boldsymbol{\xi} = (\xi, \eta)$ and $\|J\|$ is its Frobenius norm.

The value of the mean ratio Jacobian at any point $\mathbf{P}_0$ of the parametric domain is a shape quality metric for the infinitesimal triangle formed by two isoparametric curves of the physical domain passing through the point $\mathbf{P}'_0 = \mathbf{S}(\mathbf{P}_0)$, as illustrated in Fig. 8. In contrast to the scaled Jacobian, that represents a quality of the mapping $\mathbf{S}$ in the sense of the orthogonality of its isoparametric curves, the mean ratio Jacobian represents both: a quality of the mapping in the sense of the orthogonality and uniformity of its isoparametric curves. Scaled Jacobian attains its maximum value 1 at the given point if the mapping conserves orthogonality of the isoparametric curves. Mean ratio Jacobian is equal 1 at the point $\mathbf{P}_0$ if the mapping conserves

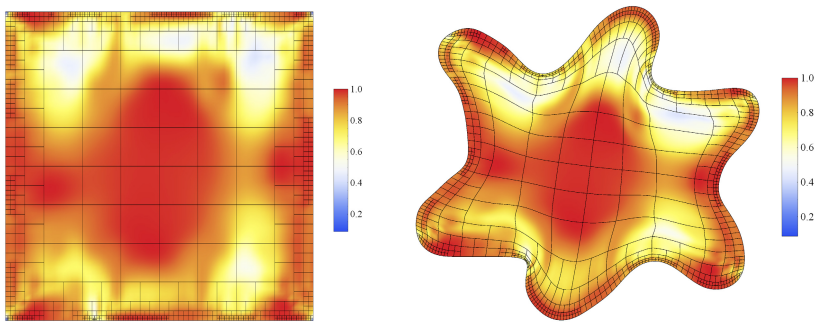

(a) (b)

Fig. 10 *Spot* test model with 844 cells, 1456 control points and 13504 quadrature points. (a) Color map of the mean ratio Jacobian of the parametric transformation represented in the parametric domain; (b) color map of the mean ratio Jacobian in the physical domain.

orthogonality and produces the same length distortion in both parametric directions, i.e., the mapping is conformal at this point.

It is easy to see that $\forall \boldsymbol{\xi}: \quad 0 \leq |J_r(\boldsymbol{\xi})| \leq |J_s(\boldsymbol{\xi})| \leq 1$, where $J_s = \frac{\det(J)}{\|\mathbf{S}_\xi\| \, \|\mathbf{S}_\eta\|}$ is scaled Jacobian.

6.2 Adaptive Refinement

Parameterization of complex geometries entails a severe distortion that can lead to appearance of low quality cells, even cells with negative Jacobian. This can be explained by the lack of degrees of freedom provided by the inner nodes. In order to improve the mesh quality in this case, we propose an adaptive strategy that refines all the cells with low quality. A similar idea was implemented for tetrahedral meshes in [9].

We proceed as follows. For each cell of the mesh, the mean ratio Jacobian is calculated at Gauss quadrature points. We use $16 = 4 \times 4$ quadrature points per cell. A cell $\hat{\Omega}_e$ is marked to refine if, at least, one of its quadrature points has mean ratio Jacobian less than a certain threshold δ. The refined T-mesh is optimized again and the process is repeated until a satisfactory mesh quality is obtained. Fig. 9 illustrates the efficacy of the proposed strategy. Additional refinements were applied to Gran Canaria Island domain with $\delta = 0.2$. The initial mesh with 3439 cells produces a T-spline parametric mapping with low quality in some areas and negative Jacobian in the North East part of the island. After adaptive refinement we have a mesh with 3577 cells and positive Jacobian in all the domain. Moreover, the minimum value of mean ratio Jacobian at the quadrature points is 0.21.

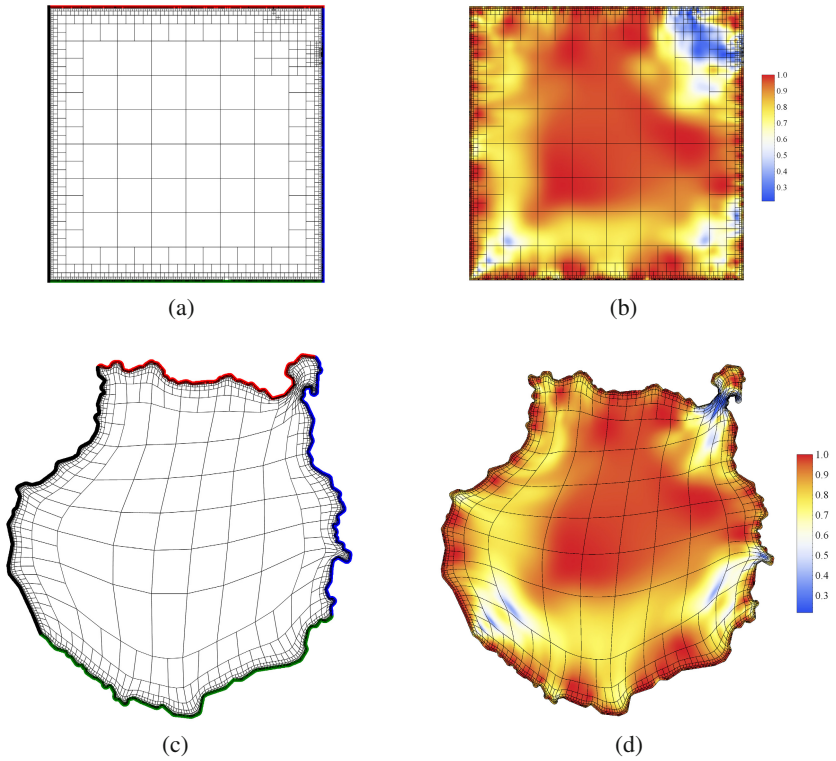

Fig. 11 Gran Canaria Island geometry with 3577 cells and 6054 control points. (a) Parametric T-mesh; (b) color map of the mean ratio Jacobian in the parametric domain; (c) physical T-mesh; (d) T-spline representation and color map of the mean ratio Jacobian in the physical domain.

7 Results and Applications

7.1 Geometric Modeling Results

The proposed algorithm was tested on several 2D domains. For all of them, we have obtained parametric mappings of high quality suitable for isogeometric analysis. In this section we present some results of the application of the method.

Fig. 10 shows the resulting T-spline representation of the *Spot* test model and the color map of the mean ratio Jacobian, represented in parametric and physical domains. As it was described in section 6, we have analyzed the quality of the parametric mapping by evaluating the mean ratio Jacobian at the quadrature points of each cell. In this case, no adaptive refinement was necessary.

Fig. 11 shows the physical T-mesh, the T-spline representation and the color map of the mean ratio Jacobian of the Gran Canaria Island geometry presented in previous section. We have constructed the adapted T-mesh starting from an initial uniform

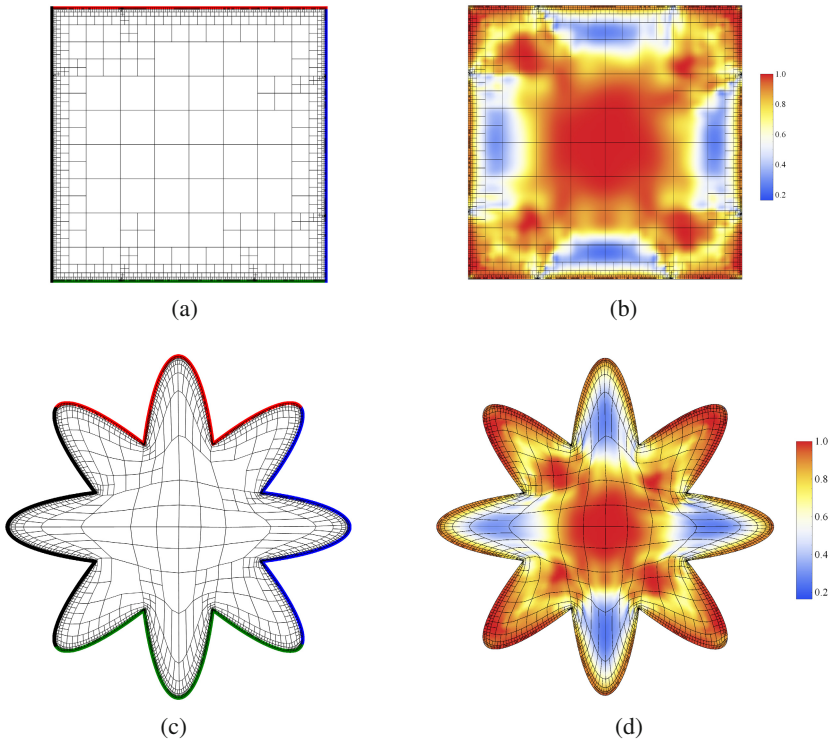

Fig. 12 Flower geometry with 2323 cells and 3935 control points. (a) Parametric T-mesh; (b) color map of the mean ratio Jacobian in the parametric domain; (c) physical T-mesh; (d) T-spline representation and color map of the mean ratio Jacobian in the physical domain.

8×8 mesh. Adaptive refinements were applied in order to improve the mesh quality in some areas with high distortion. In particular, three iterations were necessary to obtain a parametric mapping with mean ratio Jacobian greater than $\delta = 0.2$ in all quadrature points.

Another example is shown in Fig. 12. In this case, one adaptive refinement was necessary to reach a mean ratio Jacobian greater than $\delta = 0.15$ in all quadrature points.

8 Conclusions and Challenges

We have proposed a new effective technique for obtaining a single T-spline parameterization of 2D geometries for the application of isogeometric analysis. A new T-mesh untangling and smoothing procedure have been applied in order to define an isomorphic transformation between parametric and physical T-mesh. Presented technique is simple and easy to implement. The algorithm have been tested in several 2D geometries and, for all of them, we have obtained a high quality parametric

transformation between the object and the parametric domain. To asses the quality of the parametric mapping, we evaluate its mean ratio Jacobian. Thereby, we detect the areas with low quality and perform an adaptive refinement in order to increase the degree of freedom in the areas with high distortion. This strategy allows to obtain a parameterization suitable for analysis with no negative Jacobian, even for complex geometries.

All the geometries presented in this work have been parameterized with the unit square. As a next step, we plan on overcome this limitation and to develop an algorithm to parameterize a 2D object with more complex polygon-type parametric domain that fits better the geometry. Also, in future research we expect to extend the presented method to 3D.

Acknowledgements. This work has been supported by the Spanish Government, "Secretaría de Estado de Universidades e Investigación," "Ministerio de Economía y Competitividad," and FEDER, grant contracts: CGL2011-29396-C03-01 and CGL2011-29396-C03-03; "Junta Castilla León," grant contract: SA266A12-2. It has been also supported by CONACYT-SENER ("Fondo Sectorial CONACYT SENER HIDROCARBUROS," grant contract: 163723).

References

[1] Bazilevs, Y., Calo, V.M., Cottrell, J.A., Evans, J.A., Hughes, T.J.R., Lipton, S., Scott, M.A., Sederberg, T.W.: Isogeometric analysis: Toward unification of computer aided design and finite element analysis. In: Trends in Engineering Computational Technology, pp. 1–16. Saxe-Coburg Publications, Stirling (2008)

[2] Bazilevs, Y., Calo, V.M., Cottrell, J.A., Evans, J.A., Hughes, T.J.R., Lipton, S., Scott, M.A., Sederberg, T.W.: Isogeometric analysis using T-splines. Comput. Meth. Appl. Mech. Eng. 199, 229–263 (2010)

[3] Branets, L., Graham, F.C.: Smoothing and adaptive redistribution for grids with irregular valence and hanging nodes. In: Proc. of the 13th International Meshing Roundtable, vol. 19-22, pp. 333–344. Springer, Berlin (2004)

[4] Cascón, J.M., Montenegro, R., Escobar, J.M., Rodríguez, E., Montero, G.: A new *meccano* technique for adaptive 3-D triangulation. In: Proc. of the 16th International Meshing Roundtable, pp. 103–120. Springer, Berlin (2007)

[5] Cascón, J.M., Montenegro, R., Escobar, J.M., Rodríguez, E., Montero, G.: The meccano method for automatic tetrahedral mesh generation of complex genus-zero solids. In: Proc. of the 18th International Meshing Roundtable, pp. 463–480. Springer, Berlin (2009)

[6] Coons, S.A.: Surfaces for computer aided design. Springfield (1964)

[7] Cottrell, J.A., Hughes, T.J.R., Bazilevs, Y.: Isogeometric analysis: Toward integration of CAD and FEA. John Wiley & Sons, Chichester (2009)

[8] Escobar, J.M., Rodríguez, E., Montenegro, R., Montero, G., González-Yuste, J.M.: Simultaneous untangling and smoothing of tetrahedral meshes. Comput. Meth. Appl. Mech. Eng. 192, 2775–2787 (2003)

[9] Escobar, J.M., Montenegro, R., Montero, G., Rodríguez, E., González-Yuste, J.M.: Smoothing and local refinement techniques for improving tetrahedral mesh quality. Computers & Structures 83, 2423–2430 (2005)

[10] Escobar, J.M., Rodríguez, E., Montenegro, R., Montero, G., González-Yuste, J.M.: SUS Code: Simultaneous mesh untangling and smoothing code (2010), http://www.dca.iusiani.ulpgc.es/proyecto2012-2014/html/Software.html
[11] Escobar, J.M., Cascón, J.M., Rodríguez, E., Montenegro, R.: A new approach to solid modeling with trivariate T-splines based on mesh optimization. Comput. Meth. Appl. Mech. Eng. 200, 3210–3222 (2011)
[12] Escobar, J.M., Montenegro, R., Rodríguez, E., Cascón, J.M.: The meccano method for isogeometric solid modeling and applications. Engineering with Computers, 1–13 (2012) (published online), doi:10.1007/s00366-012-0300-z
[13] Farin, G., Hansford, D.: Discrete Coons patches. Comput. Aid. Geom. Design 16, 691–700 (1999)
[14] Freitag, L.A., Knupp, P.M.: Tetrahedral mesh improvement via optimization of the element condition number. Int. J. Num. Meth. Eng. 53, 1377–1391 (2002)
[15] Freitag, L.A., Plassmann, P.: Local optimization-based simplicial mesh untangling and improvement. Int. J. Num. Meth. Eng. 49, 109–125 (2000)
[16] Knupp, P.M.: Algebraic mesh quality metrics. SIAM J. Sci. Comput. 23, 193–218 (2001)
[17] Knupp, P.M.: A method for hexahedral mesh shape optimization. Int. J. Num. Meth. Eng. 58(2), 319–332 (2003)
[18] Li, B., Li, X., Wang, K.: Generalized polycube trivariate splines. In: SMI 2010, International Conference of Shape Modeling and Applications, pp. 261–265 (2010)
[19] Li, X., Guo, X., Wang, H., He, Y., Gu, X., Qin, H.: Harmonic volumetric mapping for solid modeling applications. In: Proc. of ACM Solid and Physical Modeling Symposium, pp. 109–120. Association for Computing Machinery, Inc. (2007)
[20] Martin, T., Cohen, E., Kirby, R.: Volumetric parameterization and trivariate B-spline fitting using harmonic functions. Comput. Aid. Geom. Design 26, 648–664 (2009)
[21] Montenegro, R., Cascón, J.M., Escobar, J.M., Rodríguez, E., Montero, G.: An automatic strategy for adaptive tetrahedral mesh generation. Appl. Num. Math. 59, 2203–2217 (2009)
[22] Montenegro, R., Cascón, J.M., Rodríguez, E., Escobar, J.M., Montero, G.: The meccano method for automatic three-dimensional triangulation and volume parametrization of complex solids. In: Developments and Applications in Engineering Computational Technology, pp. 19–48. Saxe-Coburg Publications, Stirling (2010)
[23] Wang, W., Zhang, Y., Liu, L., Hughes, T.J.R.: Trivariate solid T-spline construction from boundary triangulations with arbitrary genus topology. Computer-Aided Design 45, 351–360 (2013)
[24] Xu, G., Mourrain, B., Duvigneau, R., Galligo, A.: Parametrization of computational domain in isogeometric analysis: Methods and comparison. Comput. Meth. Appl. Mech. Eng. 200, 2021–2031 (2011)
[25] Xu, G., Mourrain, B., Duvigneau, R., Galligo, A.: Variational harmonic method for parameterization of computational domain in 2D isogeometric analysis. In: 12th International Conference on Computer-Aided Design and Computer Graphics, pp. 223–228. IEEE, Jinan (2011)
[26] Zhang, Y., Wang, W., Hughes, T.J.R.: Solid T-spline construction from boundary representations for genus-zero geometry. Comput. Meth. Appl. Mech. Eng. 249-252, 185–197 (2012)